ISBN: 978-3-95450-132-8 doi:10.18429/JACoW-IPAC2014-MOPRI029

SPECTROMETER FOR LASER-PULSED ELECTRONS FROM FIELD EMISSION CATHODES

S. Mingels*, V. Porshyn, B. Bornmann, D. Lützenkirchen-Hecht, G. Müller
University of Wuppertal, FB C Physics Department, Gaußstraße 20, 42119 Wuppertal, Germany

Abstract

In order to develop highly brilliant, pulsed electron sources based on photo-induced field emission, which might combine the advantages of photo and field emission, a novel measurement system with electron spectrometer was constructed. The electrons are extracted from a cold cathode by a mesh gate under pulsed laser illumination (3.5 ns, 10 Hz, 0.5-5.9 eV, > 0.3 mJ). The system was upgraded with a high resolution spectrometer that can handle electron pulses. Further system extensions enabling temperature monitoring of the cathode unit, precise positioning of both cathodes and gates as well as their dust protected insertion at the load lock were installed. The spectrometer commissioning was carried out with a W-tip, which yielded a reliable work function value and an energy resolution < 33 meV.

INTRODUCTION

Future radiation sources like free electron lasers (FEL) require highly brilliant electron beams from pulsed sources [1]. Actually alkali-based photocathodes (e.g. Cs_2Te) are used which provide extremely high peak currents (< 50 A) in short pulses (~20 ps). However, their utility is limited by the thermal emittance (1 mm mrad) and lifetime (about 1 month for ultra-high vacuum (UHV) below 10^{-8} Pa) [2].

An attractive alternative for highly brilliant and robust electron sources is photo-induced field emission (PFE) which might combine the fast switching of PE with the low emittance of FE [3]. Therefore, we report here on major extensions of our UHV PFE system [4] for the systematic investigation of flat cathodes under high electric field and ns-pulsed tunable laser illumination. First quantum efficiency (QE) measurements of Au and Ag crystals as well as n-Si, p-Si, and GaN wafers revealed PE resonances at specific energies and first hints for PFE in case of Ag [5,6]. However, a clear identification of the emission type was not possible mainly because of the lack of pulsed electron spectra and parasitic FE from particulates.

SYSTEM LAYOUT

The actual PFES system (Fig. 1) consists of a load-lock and the main chamber with a base pressure of 10^{-5} Pa and 10^{-7} Pa, respectively. The laminar air flow box and curtains around the load-lock provide ISO class 5 conditions for the exchange of samples and gates. Beside the linear transfer system, an Ar^+ ion source is installed in the load-lock which enables in situ sample cleaning.

*Contact: s.mingels@uni-wuppertal.de

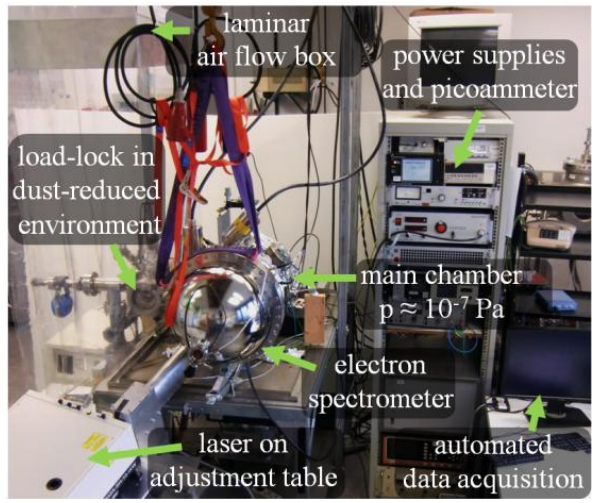

Figure 1: Photo of the PFES system.

The main chamber contains the triode system with cathode, gate, and spectrometer. The left photo in Fig. 2 shows that a part of the cathode sample opposite to the Cu mesh gate (Ø ~3 mm, 18 µm thick, 85% opt. transmission) can be exposed to both high electrostatic fields E and laser pulses of energy $h\nu$, and that a part of the extracted PFE electrons will be picked up by the spectrometer. In the right photo of Fig. 2, important extensions of the cathode unit can be seen, i.e. two piezo-driven tables for xy-positioning (18×18 mm^2 in 200 nm steps) in addition to the z-piezo (38 µm range) and two temperature sensors. T is varied by LN_2-cooling (> 77 K) or heating (< 400 K) through the support rod, which can also be retracted over 40 mm for in situ sample exchange.

A dc power supply provides a gate voltage (V_{gate}< +20 kV) and cathode current (I < 1 mA) which is measured with a Keithley® 6485 picoammeter. In order to push the electrons into the grounded spectrometer, the cathode is biased (V_{bias} = -100-0 V). By means of two screws, a double periscope for orthogonal directions and a long-range microscope, the tilt between gate and cathode can be in situ reduced (< 20 µm) for a gap Δz < 1 mm. Accordingly the applied extraction field is determined by $E = (V_{gate} - V_{bias})/\Delta z$.

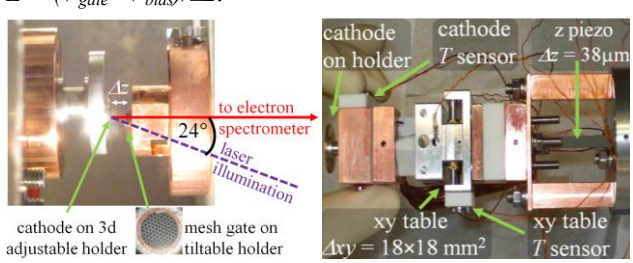

Figure 2: Top view of the cathode-gate configuration in measurement position (left) and new cathode unit (right).

ISBN: 978-3-95450-132-8 doi:10.18429/JACoW-IPAC2014-MOPRI029

The kinetic energy W of the gate-transmitted electrons is measured with a spectrometer (Specs® Phoibos 100) which consist of a high-acceptance nozzle, hemispherical sector analyzer (180°, 100 mm mean radius R) and a detector unit. In order to shield the electrostatic lenses of the nozzle against the strong E of the gate, a highly transparent mesh is used as shown in Fig. 3. Electron trajectory calculations with COMSOL® Multiphysics reveal that field penetration leads to V_{gate}-dependent electron focusing, which strongly reduces the acceptance and resolution of the spectrometer. There are four operation modes of the electrostatic lenses in the nozzle: high transition (HT) for high count rates, lateral magnification (LM) for high sample resolution, angular dispersion (AD) for angle-resolved measurements, and acceleration mode (AM) for low energy spectroscopy. Moreover, the acceptance of electrons can be reduced by means of an iris with adjustable aperture of d_{iris} = 2-27 mm. The accepted electrons are focused on mode-dependent entrance slits of different shape: curved (R = 100 mm) with slit width d_{slit} of 0.05, 0.2, 0.8, 3.0, or 7.0 mm for HT, circular with Ø 1 or 3 mm for LM, and straight with d_{slit} = 2 mm for AD modes.

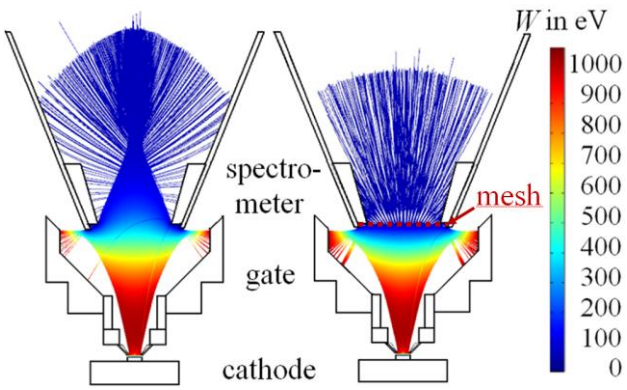

Figure 3: Electron trajectories for a -50 V biased cathode, 1 kV gate voltage and grounded spectrometer without (left) and with (right) mesh at nozzle entrance.

The retarding potential at the entrance slit is adjustable to the pass energy W_{pass} (0 - 660 eV) of the electrostatic analyzer, which determines the energy window (±10% of W_{pass}) and the maximum energy resolution (2×10^{-4} of W_{pass}) of the spectrometer, which is for the narrowest slit also limited by the divergence to about 7 meV. In contrast to the previously used scanning spectrometer with equal entrance and exit slits [4], the spectra are obtained with a 2D detector unit. It consists of a chevron-type multi-channel plate (MCP), a cathodoluminescent screen (CS) and a charge-coupled device (CCD) camera. The MCP (active electrode Ø 42 mm, thickness 0.5 mm, channel Ø 10 µm, transmission > 57%) provides a gain of 6.5×10^7. The CS (100 µm thick Gd_2O_2S:Tb) yields visible light (1.8-3.4 eV) with a afterglow time (90-10%) of 1 ms. The final image resolution is determined by the CCD sensor (1392×1024 pixels of 6.45 µm^2 size, single shot counts 12 bit, 20 MHz). Accordingly, this detector unit can be operated in a snap shot mode (SSM) which is suitable even for the detection of single laser-pulsed spectra. Nevertheless, spectra can be averaged to improve the signal-to-noise ratio.

The system control and data acquisition is performed by LabView® software. A trigger signal is used to synchronize the laser with the readout of the picoammeter and the CCD camera. Beside I and the CCD images, the actual V_{gate}, T of sample and support rod are recorded.

SPECTROMETER COMISSIONING

In order to check the limits of the extended PFE system, first measurements were performed in the snap shot mode with a well-defined tungsten tip emitter shown in Fig. 4. It was electrochemically etched from a wire in KOH and in situ heated by a FE current of 1 µA for more than 30 min, resulting in an average radius of about 10 µm. The tip had a height of 3.1 mm above its holder plate and was concentrically positioned in front of the mesh gate at Δz = 300 µm, which yields an effective field enhancement factor β of at least some hundred. The I-V_{gate} curve was measured between 1040 V and 1070 V in 1 V steps resulting in 10-20 nA. As expected, a Fowler-Nordheim (FN) like I-E dependence was reproducibly obtained (Fig. 5). The resulting β-values above 1000, however, can only be explained by the presence of the sharp edges.

A wide-energy high count rate spectrum was acquired using the snap shot mode to minimize influences of current fluctuations. The cathode was biased with V_{bias} = -93 V and V_{gate} = 951 V was applied which resulted in I = 13 nA. In order to achieve a proper signal-to-noise ratio for this low current a wide slit with d_{slit} = 7 mm, d_{iris} = 27 mm, and W_{pass} = 10 eV were chosen. 20 images with a CCD detector dwell time of 1 s were averaged. Figure 6 (top) shows raw data from the CCD detector for one snap shot on the left. As expected a peak appears rather sharp at the Fermi level W_F for the tip. In order to get the normalized energy spectrum the angular dispersive axis was accumulated. The result plotted versus W-W_F in Figure 6 (bottom), which reveals on first sight a FN-like spectrum. Fitting of the left slope combined with the FN-plot in Fig. 2 leads to a Φ value of 4.42 ± 0.19 eV, which is in fair agreement with the literature value of 4.55 eV [7]. Furthermore, fitting the right slope with the Fermi

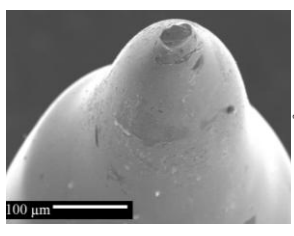

Figure 4: SEM image of the used tungsten tip with some sharp edges.

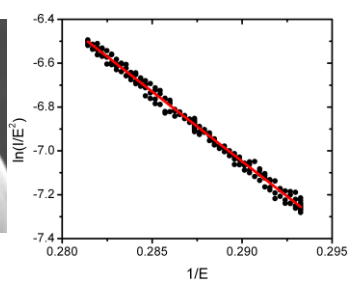

Figure 5: FN-plot of the dc FE from the tungsten tip. The red line is the best fit to FN theory.

ISBN: 978-3-95450-132-8 doi:10.18429/JACoW-IPAC2014-MOPRI029

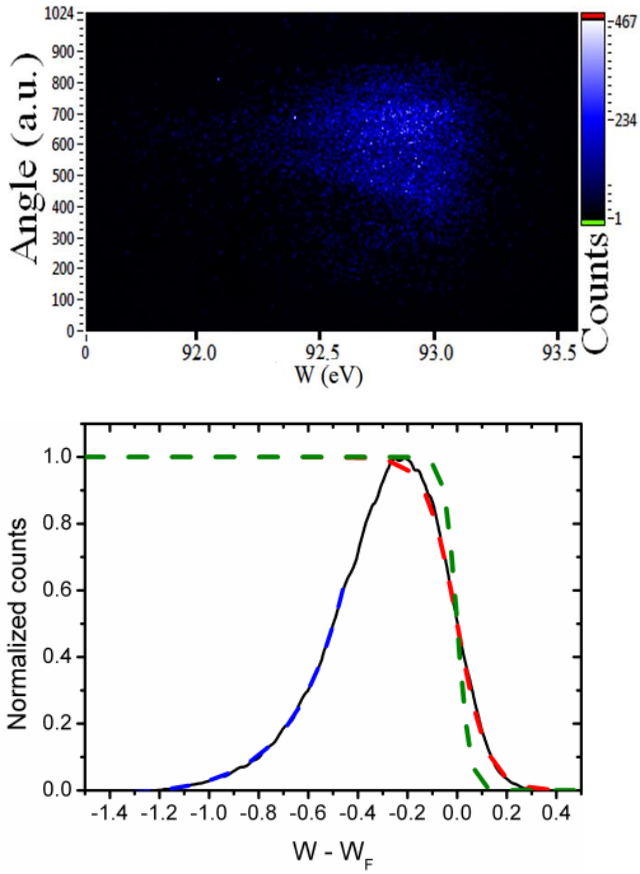

Figure 6: CCD image of a FE spectrum from the W tip for I = 13 nA (top) with the resulting spectrum (bottom). The blue line is the exponential FN fit, and the red (green) line shows the Fermi function for T = 720 (300) K.

function $F(W,T)$ yields the T value of the emitting surface. Since this fit reveals a high T value of about 720 K despite the rather low current it is likely that the spectrometer resolution with the chosen configuration was not high enough to observe the real Fermi edge or an unexpected strong emitter heating occurred. Accordingly, one high resolution spectrum, which is shown in Figure 7, for a low current of 4 nA was recorded with d_{slit} = 0.05 mm, W_{pass} = 10 eV, and d_{iris} = 2 mm. The spectrum appears quite noisy which hinders a proper fit of the right slope with $F(W,T)$. Especially, the tail is slightly smeared out by the noise level of the detector unit due to the low count rates. Hence, $F(W,300\ \mathrm{K})$ was plotted in Figure 7 leading to a good accordance with the measured right slope. Furthermore, from this edge the resolution can be estimated to be better than 33 meV. To get a lower upper bound a sharper edge in a spectrum is necessary, which can obtained e.g. for FE from a cooled tungsten tip.

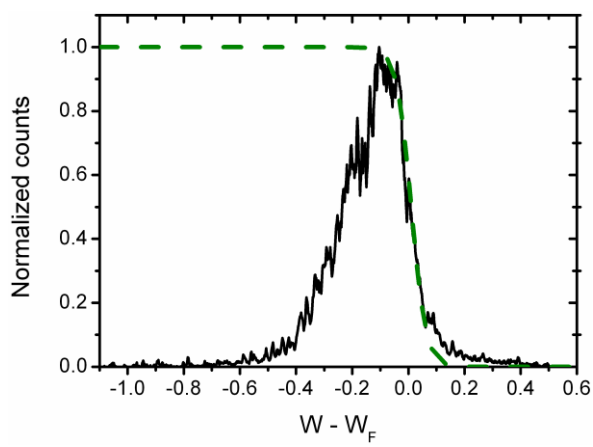

Figure 7: High resolution spectrum of the W tip for I = 4 nA (dashed green line: Fermi function for T = 300 K).

CONCLUSION AND OUTLOOK

Comprehensive extensions of the PFE spectrometer system were performed with an improvement of the triode system. It includes the installation of an xy table for lateral cathode positioning, heating and cooling of the support rod and sensors for T control as well as a double periscope, long range microscope, and tiltable gate for in situ gap tilt control. A dust free environment at the load-lock helps to avoid dust contamination during the sample insertion. The focus of the system improvement lied on the installation of a spectrometer with 2D detector unit for pulsed operation. For commissioning an integral I-V_{gate} curve spectrum and a wide energy high count rate image from a W tip was measured yielding FN like behavior and a reasonable Φ value, respectively. Finally, a high resolution spectrum of the same emitter was obtained which yielded an analyzer resolution better than 33 meV.

First measurements of laser-pulsed spectra are planned with well-defined flat Ag and Au crystals. After that the search for PFE will be concentrated on direct, wide band gap, and highly doped semiconductors which might serves as high-QE PFE cathodes. As soon as a promising PFE source is found, its emittance should be measured at DESY Zeuthen or FZR Dresden.

ACKNOWLEDGMENT

This project is funded by the German Federal Ministry of Education and Research (BMBF) under the project numbers 05K10PXA and 05K13PX2.

REFERENCES

[1] D.H. Dowell et al., Nucl. Instr. Meth. Phys. A 622, 685 (2010).
[2] A.M. Altarelli et al., The European X-Ray Free-Electron Laser, Technical design report, DESY 2006-097 (2007).
[3] C.A. Brau, Nucl. Instrum. Methods Phys. Res. A 393, 426 (1997).
[4] B. Bornmann et al., Rev. Sci. Instrum. 83, 013302 (2012).
[5] S. Mingels et al., FEL'13, New York, USA, August 2013, p. 339, (2013); http://www.JACoW.org
[6] R. Schreiner et al., IVNC'13, Roanoke, USA, July 2013, (2013), http://ieeexplore.ieee.orgCRC
[7] B.J. Hopkins and J.C. Rivière, Proc. Phys. Soc. 81, 590 (1963).